A hydraulic model for flow rate ratio of triple cannulation extracorporeal membrane oxygenation ⊘

Fan Wu (吴凡); Hongping Wang (王洪平); Chunyu Wang (王春雨); ... et. al

Check for updates

View Online   Export Citation   CrossMark

Articles You May Be Interested In

Comparison of single-stage and multi-stage drainage cannula flow characteristics during venoarterial extracorporeal membrane oxygenation

Physics of Fluids (February 2023)

Vortex dynamics of veno-arterial extracorporeal circulation: A computational fluid dynamics study

Physics of Fluids (June 2021)

Flow patterns of blood post-application of cross-clamp during cardiopulmonary bypass

Physics of Fluids (December 2022)
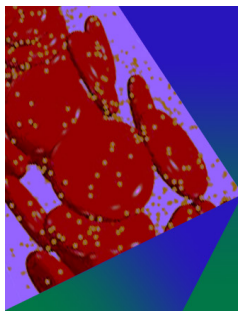
Physics of Fluids

Special Topic: Flow and Forensics

Submit Today!

AIP Publishing

A hydraulic model for flow rate ratio of triple cannulation extracorporeal membrane oxygenation

View Online   Export Citation   CrossMark

Fan Wu (吴凡),[1,2] ⬡ Hongping Wang (王洪平),[1,2] ⬡ Chunyu Wang (王春雨),[1,2] ⬡ Duo Xu (徐多),[1,2] ⬡ and Shizhao Wang (王士召)[1,2,a] ⬡

AFFILIATIONS

[1]LNM, Institute of Mechanics, Chinese Academy of Sciences, Beijing 100190, China
[2]School of Engineering Sciences, University of Chinese Academy of Sciences, Beijing 100049, China

[a]Author to whom correspondence should be addressed: wangsz@lnm.imech.ac.cn

ABSTRACT

Triple cannulation extracorporeal membrane oxygenation (ECMO) provides advanced life support to patients with respiratory and hemodynamic failure by replacing the function of the heart and lungs. The application of triple cannulation ECMO suffers from the difficulty in predicting the flow rate ratios of the cannulas. We address this difficulty by proposing a hydraulic model, where the effects of the triple cannulation are modeled by head losses in a bifurcated tube. The proposed model correctly predicts the flow rate ratios and quantitatively captures the effects of geometrical parameters. This model can help to configure the cannula pair for clinical practices and interventional therapy.

Published under an exclusive license by AIP Publishing. https://doi.org/10.1063/5.0088186

The investigation of the flow rate ratio in this Letter is motivated by the advanced application of extracorporeal membrane oxygenation (ECMO). ECMO is an extracorporeal machine that replaces the function of the heart and/or lungs of a patient to provide life support through cannulas (plastic tubes).[1] ECMO is conventionally used with dual cannulation (cannulation of two large vessels) in which ECMO pumps the deoxygenated blood from a vein to an artificial lung through a cannula and sends the oxygenated blood back into a vein (V-V ECMO) or an artery (V-A ECMO) through another cannula.[2] According to the report of Extracorporeal Life Support Organization, ECMO has successfully helped 58% of the registry to hospital discharge during 1989–2016.[3] ECMO also successfully supports the patients with coronavirus disease 2019 (COVID-19).[4]

Recently, a new hybrid cannulation is proposed by adding a third cannula to an existing V-V or V-A ECMO.[5] This new hybrid cannulation is termed as the triple cannulation, which represents a novel and complex form of mechanical support.[6] The triple cannulation ECMO has been shown to be a feasible technique in treating patients with combined respiratory and hemodynamic failure.[7] Given that the triple cannulation is featured by a bifurcated tube that connects three vessels, the two branches of the bifurcated tube should be carefully configured to obtain the desired flow rates into the venous and arterial cannulas, respectively.[6]

Despite the increasing clinical use of the triple cannulation ECMO, there are a few model to predict the flow rates in the two branches of the bifurcated tube. Belliato *et al.*[6] carried out the first experiment based on a physical *ex vivo* proxy of the triple cannulation ECMO without throttle valve, which helps to avoid hemolysis.[8] They proposed a computational spreadsheet based on the experimental data to predict the flow rates. The prediction of the flow rates helps to configure the cannula pair for clinical practices and interventional therapy. However, the prediction of the flow rates in the two branches of a bifurcated tube is not trivial, since the flow in a tube depends on both geometrical parameters, such as curvature and cross section area,[9–11] and fluid dynamic parameters, such as Reynolds number and boundary condition.[12–14] Particularly, it is of great challenge to evaluate the effects of geometrical parameters on the flow rates. Although the flows in the bifurcated tube have been successfully investigated by using different models for the biological[15–17] and mechanical[18,19] systems, we have not found any theoretical model taking into account of the geometrical and physical features of the triple cannulation ECMO.

In this Letter, we propose a theoretical model for the triple cannulation ECMO. The proposed model is constructed based on the hydraulic theory, and it can compute the flow rates in the two branches of the bifurcated tube. The theoretical model employees the physical *ex vivo* proxy of Belliato *et al.*,[6] which reflects the geometrical

features of the triple cannulation ECMO. We model the effects of the geometrical features, such as bifurcation, bendiness, and contraction of the tube, by the head losses (specific energy losses divided by the gravity acceleration) in the tube, in a similar way in constructing the reduced-order model for the cardiovascular system.[20–22] Therefore, the proposed model can also evaluate the effects of geometrical parameters on the flow rates.

The schematic of the physical *ex vivo* proxy of the triple cannulation ECMO[6] is shown in Fig. 1. The flow from the oxygenator to cannulas is modeled as a bifurcated tube with two branches. We refer the two branches as the arterial branch and venous branch, since they connect to an artery and a vein, respectively. The arterial branch consists of an arterial pipe (the part of tube outside of the body) and an arterial cannula (the part of the tube to be inserted into the body). The length and inner diameter of the arterial pipe are L_{ap} and D_{ap}, respectively. The length and inner diameter of the arterial cannula are L_{ac} and D_{ac}, respectively. Hereinafter, we use the subscripts "p" and "c" to denote the variables associated with pipe and cannula, respectively, and use the subscripts "a" and "v" to represent the variables associated with the arterial branch and venous branch, respectively. The arterial pipe and arterial cannula are connected by an arterial tapered tube with an angle of θ_{at}. The venous branch consists of a venous pipe with a length of L_{vp} and an inner diameter of D_{vp} and a venous cannula with a length of L_{vc} and an inner diameter of D_{vc}. The venous pipe and venous cannula are connected by a venous tapered tube with an angle of θ_{vt}. The two branches are connected to a Y-connector with the inner diameter of D_p and length of L_b. We set $D_p = D_{ap} = D_{vp}$ in the current work according to the setups of Belliato *et al.*[6] The angle between the trunk pipe and the branch is θ_b. The bendiness of each branch is modeled by elbows with different angles θ_{ae1}, θ_{ae2}, and θ_{ve} according to the diagram of Belliato *et al.*[6] The pressure difference between the outlets of the two branches is given by the height difference H_a according to the setups of Belliato *et al.*[6] More details of the physical *ex vivo* proxy of the triple cannulation ECMO can be found in the supplementary material.
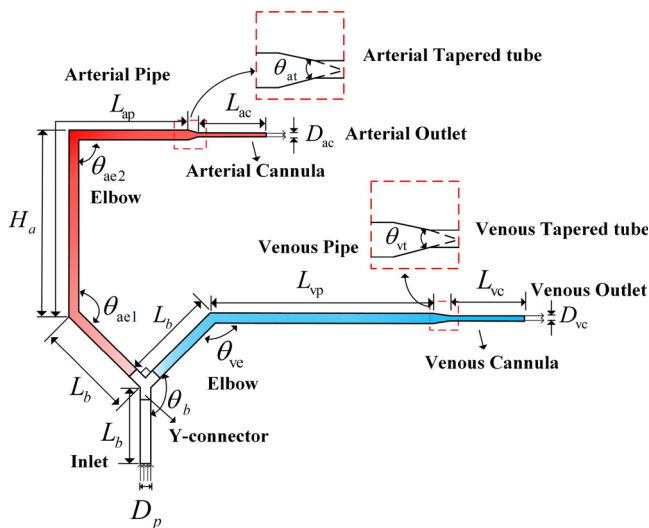

FIG. 1. Schematic of the physical *ex vivo* proxy of the triple cannulation ECMO from the oxygenator to cannulas (not to scale).

We introduce the flow rate ratio (β_v) defined as the ratio of the flow rate in the venous branch (Q_v) to the total flow rate (Q_{tot}) for the convenience of discussion, namely, $\beta_v = Q_v/Q_{tot}$. The flow rates in the arterial and venous branches can be easily computed by using the flow rate ratio (β_v) and the total flow rate (Q_{tot}). We propose a hydraulic model as follows to compute the flow rate ratio β_v:

$$\frac{1}{\pi^2 D_{ac}^4}(1-\beta_v)^2 - \frac{1}{\pi^2 D_{vc}^4}\beta_v^2$$
$$= \frac{g}{8Q_{tot}^2}\left(h_{Lv} + h_{fv} - h_{La} - h_{fa} + \frac{p_v - p_a}{\rho g} - H_a\right), \quad (1)$$

where g is the gravity acceleration, h_{La} and h_{Lv} are the total local losses in arterial and venous branches, respectively. h_{fa} and h_{fv} are the total friction losses in arterial and venous branches, respectively. p_a and p_v are the pressure at the outlet of arterial and venous branches, respectively. ρ is the fluid density.

The hydraulic model Eq. (1) is constructed based on the mass and energy conservation equations for incompressible flows. The derivation of the model is reported as follows. The mass conservation in the bifurcated tube can be described as

$$Q_{tot} = U_{vp} \times A_p + U_{ap} \times A_p, \quad (2)$$
$$\beta_v Q_{tot} = U_{vc} \times A_{vc} = U_{vp} \times A_p, \quad (3)$$
$$(1-\beta_v)Q_{tot} = U_{ac} \times A_{ac} = U_{ap} \times A_p, \quad (4)$$

where $A_p = \pi D_p^2/4$ is the cross section area of the arterial and venous pipes. U_{vp} and U_{ap} are the average velocity in the arterial and venous pipes, respectively. $A_{vc} = \pi D_{vc}^2/4$ and $A_{ac} = \pi D_{ac}^2/4$ are the cross section areas of the arterial and venous cannulas, respectively. U_{vc} and U_{ac} are the average velocity in the arterial and venous cannulas, respectively. The energy conservation of flows in the bifurcated tube can be expressed by the general Bernoulli equation for viscous flows,

$$\frac{p_{in}}{\rho g} + \frac{U_{in}^2}{2g} = \frac{p_v}{\rho g} + \frac{U_{vc}^2}{2g} + h_{Lv} + h_{fv}, \quad (5)$$

$$\frac{p_{in}}{\rho g} + \frac{U_{in}^2}{2g} = \frac{p_a}{\rho g} + \frac{U_{ac}^2}{2g} + H_a + h_{La} + h_{fa}, \quad (6)$$

where p_{in} and U_{in} are the pressure and velocity at the inlet, respectively. Combining Eqs. (2)–(6) gives

$$\frac{p_a}{\rho g} + \frac{(1-\beta_v)^2 Q_{tot}^2}{2g A_{ac}^2} + H_a + h_{La} + h_{fa} = \frac{p_v}{\rho g} + \frac{\beta_v^2 Q_{tot}^2}{2g A_{vc}^2} + h_{Lv} + h_{fv}. \quad (7)$$

Rearranging the terms in Eq. (7) gives the model of Eq. (1).

Equation (1) is a transcendental equation, since the total friction losses (h_{fa} and h_{fv}) and total local losses (h_{La} and h_{Lv}) implicitly depend on the flow rate ratio β_v. For the *ex vivo* proxy of triple cannulation ECMO, the total friction losses h_{fa} and h_{fv} can be decomposed as the friction losses from pipes (h_{fap} and h_{fvp}) and cannulas (h_{fac} and h_{fvc}),

$$h_{fa} = h_{fap} + h_{fac}, \quad (8)$$
$$h_{fv} = h_{fvp} + h_{fvc}. \quad (9)$$

The total local losses (h_{La} and h_{Lv}) are given by the summation of the local losses from bifurcation (h_{Lab} and h_{Lvb}), tapered tubes (h_{Lat} and h_{Lvt}), and elbows (h_{Lae1}, h_{Lae2}, and h_{Lve}),

TABLE I. Calculation formula of friction coefficient.

Reynolds number[a]	Theoretical or empirical formula
$Re < 2040$	$\lambda = 64Re^{-1}$
$2040 < Re < 3200$[b]	$\lambda = 0.0001157Re^{0.7352}$
$3.2 \times 10^3 < Re < 10^5$	$\lambda = 0.3164Re^{-0.25}$[c]

[a]The Reynolds number is $Re = UD/\nu$, where D is the diameter, U is the average velocity, and ν is the kinematic viscosity of the fluid.
[b]The expression of the critical region is obtained by fitting the experimental data.[23]
[c]The Blasius empirical correlation for turbulent pipe friction.[24]

TABLE II. Calculation formula of local loss coefficient.

Geometry	Local loss coefficient
Elbow[a]	$\xi_e = 0.946\sin^2\dfrac{\pi-\theta}{2} + 2.05\sin^4\dfrac{\pi-\theta}{2}$
Bifurcation[b]	$\xi_b = 1 + \beta_i^2\psi_i^2 - 2\beta_i\psi_i\cos\varphi_i$
Tapered tube[c]	$\xi_t = \dfrac{0.8\sin(\theta/2)[1-(D_i/D_p)^2]}{(D_i/D_p)^4}$

[a]θ defines the inside angle of the elbow.[25]
[b]The variables β_i and ψ_i are the flow rate ratio and area ratio of branch to trunk pipe, respectively. $\varphi_i = 3(\pi - \theta_b)/4$ is defined from the angle θ_b.[26]
[c]θ is the contraction angle as shown in Fig. 1. D_i is the diameter of cannulas.[27]

$$h_{La} = h_{Lab} + h_{Lae1} + h_{Lae2} + h_{Lat}, \quad (10)$$
$$h_{Lv} = h_{Lvb} + h_{Lve} + h_{Lvt}. \quad (11)$$

The friction loss and local loss in each part can be computed by

$$h_f = \lambda \cdot \frac{L}{D} \cdot \frac{U^2}{2g}, \quad (12)$$
$$h_L = \xi \cdot \frac{U^2}{2g}, \quad (13)$$

where D is the diameter, U is the average velocity, λ and ξ are the friction coefficient and the local loss coefficient, respectively. These coefficients can be computed using the theoretical or empirical formulations from hydraulics in Tables I and II.

TABLE III. Cannula diameters of different cases.

Case	Arterial cannula		Venous cannula	
	Outer diameter[a]	Inner diameter[b]	Outer diameter	Inner diameter
A19-V17	19 Fr	5.667 mm	17 Fr	5.000 mm
A19-V19	19 Fr	5.667 mm	19 Fr	5.667 mm
A19-V21	19 Fr	5.667 mm	21 Fr	6.333 mm
A17-V17	17 Fr	5.000 mm	17 Fr	5.000 mm
A17-V19	17 Fr	5.000 mm	19 Fr	5.667 mm
A17-V21	17 Fr	5.000 mm	21 Fr	6.333 mm

[a]The outer diameter of cannula is usually measured in the unit of Fr, where 1 Fr = 1/3 mm.
[b]The inner diameter is computed by $D_{in} = D_{out} - 2\delta_c$, where D_{out} and δ_c are the outer diameter and wall thickness, respectively. The wall thickness is 1 Fr.

We compute the flow rate ratio β_v by numerically solving Eq. (1) using the bisection method for transcendental equations[28] with the given diameters of the cannulas (D_{ac} and D_{vc}) on the left-hand-side of Eq. (1) and the flow parameters on the right-hand-side of Eq. (1). Our source code to numerical solving Eq. (1) is available for free from the GitHub link reported in the Data Availability statement.

We use the experimental measurements in Belliato *et al.*[6] to validate the proposed hydraulic model. We have computed the flow rate ratios at different total flow rates with six pairs of cannulas as shown in Table III, which ensures that the proposed model not only gives good prediction to the flow rate ratios but also helps identifying the dominant parameter that affects the flow rate ratio.

For each pair of cannulas, the flow rate ratio β_v decreases as the total flow rate Q_{tot} increases. The proposed hydraulic model correctly reflects the variation of the flow rate ratio β_v with the total flow rate Q_{tot}, as shown in Fig. 2. The maximum difference of the flow rate ratio between the model and the experimental measurements occurs in the case of A19-V19 at $Q_{tot} = 5$ L/min, where the flow rate ratio β_v predicted by the proposed model is 0.53, while that of the experimental measurement is 0.55. The relative error for this case is about 3.6%. The average error of the flow rate ratio in all the 36 cases is about 1.3%.

The proposed model can quantitatively capture the geometrical parameters that affect the flow rate ratio β_v, as shown by a typical
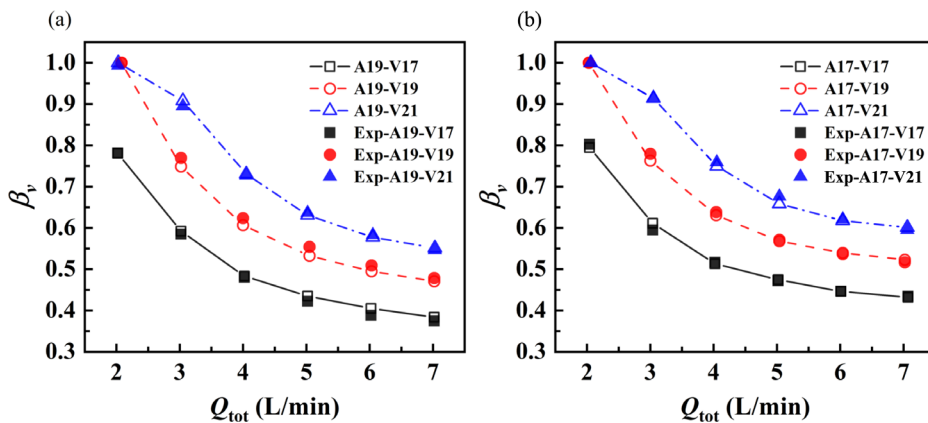
FIG. 2. Flow rate ratio β_v varies with the total flow rate Q_{tot} at different pairs of cannulas with (a) the arterial cannula diameter of 19 Fr and (b) the arterial cannula diameter of 17 Fr.
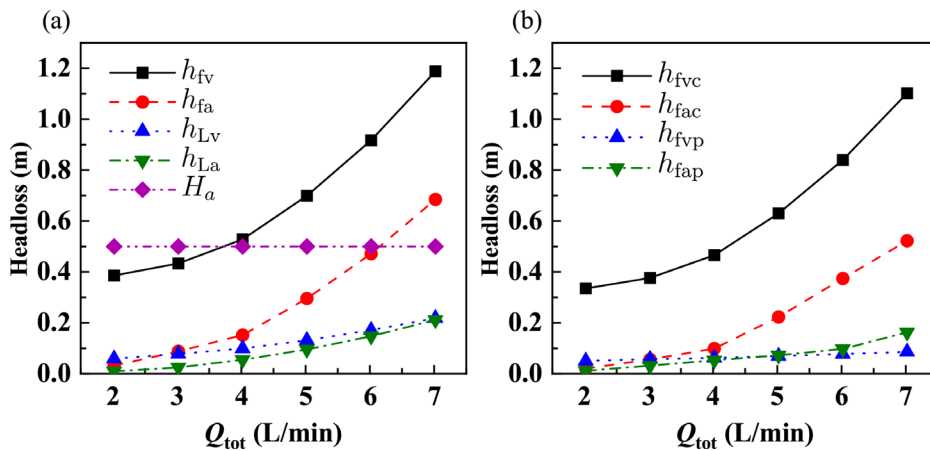
FIG. 3. Head losses in different parts of the bifurcated tube with A19-V17, (a) the total friction losses (h_{fv} and h_{fa}) and the total local losses (h_{Lv} and h_{La}) and (b) the friction losses (h_{fvc} and h_{fac}) along the cannulas and the friction losses (h_{fvp} and h_{fap}) along the pipe.

configuration of cannula pair with A19-V17. Figure 3(a) shows that the total friction losses (h_{fa} and h_{fv}) and total local losses (h_{La} and h_{Lv}) increase as the total flow rate increases. While among them, the total friction losses increase more rapidly than the total local losses. In all the cases, the sum of the h_{fv} and h_{fa} accounts for more than 81.3% of the total loss. The results clearly show that the friction loss dominants the total loss in the configuration in this study.

The proposed model can be further used to analyze the friction loss associated with different parts of the bifurcated tube by referring to Eqs. (8) and (9). The contributions of the friction loss from the pipe and cannula in each branch are shown in Fig. 3(b). We observe that both the friction losses associated with the pipe and cannula increase with the total flow rate. However, the friction loss associated with cannula increases more rapidly. The sum of the friction loss in the cannulas h_{fvc} and h_{fac} accounts for more than 83.0% of the total friction loss in all the cases in this configuration. The results show that friction loss is mainly contributed by the cannulas.

In summary, the triple cannulation ECMO is a novel and complex form of mechanical support for patients with combined respiratory and hemodynamic failure. The application of this ECMO technique encounters difficulty in clinical practices and interventional therapy due to lacking good prediction of the flow rate ratio in the triple cannulation. We address this difficulty from the viewpoint of fluid dynamics by proposing a hydraulic model, where the geometrical features of the triple cannulation are modeled using the head losses in the tube. The proposed model is validated by the physical *ex vivo* proxy of triple cannulation ECMO.[6] The flow rate ratios in 36 cases with different pairs of cannula configuration and total flow rates were computed using the proposed model. The results show that the maximum difference of the flow rate ratios predicted by the proposed model is 3.6% for all the cases investigated in this work. We show that the friction loss dominants the total loss in the triple cannulation configuration, and the friction loss is mainly contributed by the cannulas. The proposed model correctly predicts the flow rate ratios as well as quantitatively captures the effects of geometrical parameters on the flow rate ratios. To the best of the authors' knowledge, Eq. (1) is the first hydraulic model for predicting the flow rate ratio of the triple cannulation ECMO. A limitation of the current hydraulic model is that a fixed height (H_a) is used to represent a typical mean pressure difference between the artery and vein in a shocked patient.[6] In clinical scenario,

the cardiovascular flow is pulsatile, although the flow in the ECMO is tuned to be steady to avoid thrombosis.[29,30] The pulsatile cardiovascular flow corresponds to a time-dependent height $H_a(t)$ in the hydraulic model. The effects of pulsatility on the flow rate ratio should be taken into account in the follow-up work.

SUPPLEMENTARY MATERIAL

See the supplementary material for detailed parameters related to the physical *ex vivo* proxy of the triple cannulation ECMO.

AUTHOR DECLARATIONS
Conflict of Interest

The authors have no conflicts to disclose.

DATA AVAILABILITY

The data that support the findings of this study are available from the corresponding author upon reasonable request. The details of the physical *ex vivo* proxy of the triple cannulation ECMO are available in the supplementary material. Our source code to numerically solve the hydraulic model equation is available from the GitHub link https://github.com/wufanxiaozi/Hydraulic_Model_ECMO or from the corresponding author.

REFERENCES

[1] M. Alexander White and P. Eddy Fan, "What is ECMO?," Am. J. Respir. Crit. Care Med. **193**, 9–10 (2016).

[2] S. A. Conrad, L. M. Broman, F. S. Taccone, R. Lorusso, M. V. Malfertheiner, F. Pappalardo, D. Nardo, M. Belliato, L. Grazioli, R. P. Barbaro *et al.*, "The extracorporeal life support organization Maastricht treaty for nomenclature in extracorporeal life support. A position paper of the extracorporeal life support organization," Am. J. Respir. Crit. Care Med. **198**, 447–451 (2018).

[3] R. R. Thiagarajan, R. P. Barbaro, P. T. Rycus, D. M. Mcmullan, S. A. Conrad, J. D. Fortenberry, M. L. Paden *et al.*, "Extracorporeal life support organization registry international report 2016," ASAIO J. **63**, 60–67 (2017).

[4]J. Badulak, M. V. Antonini, C. M. Stead, L. Shekerdemian, L. Raman, M. L. Paden, C. Agerstrand, R. H. Bartlett, N. Barrett, A. Combes *et al.*, "Extracorporeal membrane oxygenation for COVID-19: Updated 2021 guidelines from the extracorporeal life support organization," ASAIO J. **67**, 485 (2021).

[5]L. C. Napp and J. Bauersachs, "Triple cannulation ECMO," in *Extracorporeal Membrane Oxygenation-Advances in Therapy* (InTech, 2016), pp. 79–99.

[6]M. Belliato, L. Caneva, A. Aina, A. Degani, S. Mongodi, L. Prahl Wittberg, C. Pellegrini, L. M. Broman, and G. A. Iotti, "An experimental model of veno-venous arterial extracorporeal membrane oxygenation," Int. J. Artif. Organs **43**, 268–276 (2020).

[7]F. Ius, W. Sommer, I. Tudorache, M. Avsar, T. Siemeni, J. Salman, J. Puntigam, J. Optenhoefel, M. Greer, T. Welte *et al.*, "Veno-veno-arterial extracorporeal membrane oxygenation for respiratory failure with severe haemodynamic impairment: Technique and early outcomes," Interact. Cardiovasc. Thorac. Surg. **20**, 761–767 (2015).

[8]P. Wu, Q. Gao, and P. L. Hsu, "On the representation of effective stress for computing hemolysis," Biomech. Model. Mechanobiol. **18**, 665–679 (2019).

[9]C. Zhu, J.-H. Seo, and R. Mittal, "Computational modelling and analysis of haemodynamics in a simple model of aortic stenosis," J. Fluid Mech. **851**, 23–49 (2018).

[10]M. S. Nagargoje, D. K. Mishra, and R. Gupta, "Pulsatile flow dynamics in symmetric and asymmetric bifurcating vessels," Phys. Fluids **33**, 071904 (2021).

[11]N. Freidoonimehr, M. Arjomandi, A. Zander, and R. Chin, "Effect of artery curvature on the coronary fractional flow reserve," Phys. Fluids **33**, 031906 (2021).

[12]A. Seetharaman, H. Keramati, K. Ramanathan, M. E. Cove, S. Kim, K. J. Chua, and H. L. Leo, "Vortex dynamics of veno-arterial extracorporeal circulation: A computational fluid dynamics study," Phys. Fluids **33**, 061908 (2021).

[13]C. Cox and M. W. Plesniak, "The effect of entrance flow development on vortex formation and wall shear stress in a curved artery model," Phys. Fluids **33**, 101908 (2021).

[14]J. Zhao, Y. Feng, K. Koshiyama, and H. Wu, "Prediction of airway deformation effect on pulmonary air-particle dynamics: A numerical study," Phys. Fluids **33**, 101906 (2021).

[15]S. Yang, Q. Wang, W. Shi, W. Guo, Z. Jiang, and X. Gong, "Numerical study of biomechanical characteristics of plaque rupture at stenosed carotid bifurcation: A stenosis mechanical property-specific guide for blood pressure control in daily activities," Acta Mech. Sin. **35**, 1279–1289 (2019).

[16]X. He and X. Yang, "Effects of exercise on flow characteristics in human carotids," Phys. Fluids **34**, 011909 (2022).

[17]Y. Chen, X. Yang, A. J. Iskander, and P. Wang, "On the flow characteristics in different carotid arteries," Phys. Fluids **32**, 101902 (2020).

[18]G. Li, T. Ye, S. Wang, X. Li, and R. UI Haq, "Numerical design of a highly efficient microfluidic chip for blood plasma separation," Phys. Fluids **32**, 031903 (2020).

[19]H. Liu and Y. Zhang, "Droplet formation in microfluidic cross-junctions," Phys. Fluids **23**, 082101 (2011).

[20]X. Zhang, D. Wu, F. Miao, H. Liu, and Y. Li, "Personalized hemodynamic modeling of the human cardiovascular system: A reduced-order computing model," IEEE Trans. Biomed. Eng. **67**, 2754–2764 (2020).

[21]M. Mirramezani and S. C. Shadden, "A distributed lumped parameter model of blood flow," Ann. Biomed. Eng. **48**, 2870–2886 (2020).

[22]C. Zhang, B. Lin, D. Li, and Y. Fan, "Application of multiscale coupling models in the numerical study of circulation system," Med. Novel Technol. Devices **14**, 100117 (2022).

[23]B. J. Mckeon, C. J. Swanson, M. V. Zagarola, R. J. Donnelly, and A. J. Smits, "Friction factors for smooth pipe flow," J. Fluid Mech. **511**, 41 (2004).

[24]W. H. Hager, "Blasius: A life in research and education," Exp. Fluids **34**, 566–571 (2003).

[25]J. Juan Villegas-Leon, A. Alberto Lopez-Lambrano, C. Fuentes, D. Aranda-Perez, and A. Alberto Lopez-Ramos, "A review of the methodologies for estimating the coefficient of losses in pipe curves under turbulent flow," Tecnol. Cienc. Agua **12**, 42–111 (2021).

[26]J. P. Mynard and K. Valen-Sendstad, "A unified method for estimating pressure losses at vascular junctions," Int. J. Numer. Methods Biomed. Eng. **31**, e02717 (2015).

[27]R. W. Fox, A. T. McDonald, and J. W. Mitchell, *Fox and McDonald's Introduction to Fluid Mechanics* (John Wiley & Sons, 2020).

[28]R. L. Burden and J. D. Faires, *Numerical Analysis* (PWS Publishers, 1985), pp. 46–52.

[29]W. Yin, S. K. Shanmugavelayudam, and D. A. Rubenstein, "The effect of physiologically relevant dynamic shear stress on platelet and endothelial cell activation," Thromb. Res. **127**, 235–241 (2011).

[30]A. Badheka, S. E. Stucker, J. W. Turek, and M. L. Raghavan, "Efficacy of flow monitoring during ECMO," ASAIO J. **63**, 496–500 (2017).